AIAA JOURNAL
Vol. 37, No. 3, March 1999

Chaotic Response of Panel Vibrations Forced by Turbulent Boundary Layer and Sound

L. Maestrello*
NASA Langley Research Center, Hampton, Virginia 23681

Experimental data are presented to show evidence of chaotic response of two adjacent aircraft panels forced by a turbulent boundary layer and pure tone sound. The experiments are a simulation of boundary-layer and fan noise loads on a fuselage sidewall with Reynolds number per meter of 2.85×10^5. The response of the panels is purely random and assumed linear when forced by the turbulent boundary-layer flow and clearly becomes nonlinear with the appearance of the interspersed periodic to chaotic motion when forced by the boundary layer with superimposed pure tone sound. The initial periodic response of two tori of two commensurate frequencies changes with an increase in pure tone sound level. The response of period-doubling bifurcations then makes a transition to chaos, which alternates with quasiperiodic response as the wave loses the spatial homogeneity. The objective is to demonstrate the existence of strong nonlinear effects on the structure response, which is not yet well understood.

I. Background

MOST studies of nonlinear deterministic and stochastic dynamic problems examine externally excited systems. A typical example of an externally excited system is an aircraft fuselage structure interacting with a turbulent boundary layer and jet engine noise. Periodic, aperiodic, and chaotic responses can occur along the sidewall of the fuselage structure during the acceleration from takeoff, as well as at cruise altitude. One type of load is the so-called buzz-saw noise in high-bypass-ratio turbofan engines. The present experiment is designed to simulate such loads, as well as structural nonlinear responses that result from turbulent boundary-layer flow and high-intensity sound interaction. Such experiments must be conducted in a wind tunnel with an anechoic test section to prevent standing wave formation between the test panel surface and the opposite sidewall of the tunnel. As a rule, the panel tension and curvature depend on the loading. This tension, therefore, constitutes a coupling between the loading and the response. One manifestation of this coupling is the spontaneous surface deformation of the panel, giving rise first to the regular and then to the irregular spatial patterns as the load increases.

In the previous experiments, panels with periodic nonlinear responses to sound and flows of constant or accelerated speeds and their active control were considered.[1,2] The present study simulates the abnormal processes of flow and sound loads, the unsteady loads of the boundary-layer pressure fluctuations coupled with the panel responses, and the sound radiation by the panel. Nonlinear behaviors result from increasing levels of pure tone sound as evidenced by the response changes in the panel from periodic motions to broadband chaos.

In the past, chaotic signals were not recognized as a physical behavior but were hidden in the broad view given by stochastic processes. At present, the interest is to distinguish between periodic, quasiperiodic, and nonperiodic responses.[3–6] In the experiments reported herein, the input of the acoustic load superimposed on the turbulent boundary-layer flow was gradually increased. First, the boundary-layer instability and then responses changing from periodic to quasiperiodic and finally to chaotic were observed, analogous to that reported in Refs. 7–12. This characteristic route to chaos was suggested by Sreenivasan,[10] Giglio et al.,[11] Newhouse et al.,[13] and Dowell.[14] In the experiments reported herein, the loads and responses are typical of certain aircraft maneuvers under conditions that simulate the Reynolds number of the turbulent boundary layer, the acoustic pressure signature of a turbofan engine, and the fuselage panel size. Results of the input load, panel response, and sound transmission are discussed. Specifically the discussion focuses on the turbulent boundary-layer responses with and without acoustic forcing; the panel with periodic, chaotic responses; and the acoustic pressure transmitted to the cabin side by the panel oscillations. As a rule, the panel tension and curvature depend on the input loading; therefore, this tension constitutes a coupling between loading and response.

Section II describes the experimental setup. The tools used to analyze the dynamics response are described in Sec. III, with Sec. III.A describing the turbulent boundary layer without and with added pure tone sound and Sec. III.B describing the panel responses, which change from periodic to chaotic. In Sec. IV, the correlation dimension and Lyapunov exponent are discussed. In Sec. V, the transmitted pressure is discussed, and the results and some conclusions are summarized in Sec. VI.

II. Experimental Apparatus and Instrumentation

The apparatus, an open-circuit wind tunnel, has been described at length in the study of constant and accelerated boundary-layer flow experiments.[1,2] The present experiments are conducted with two aluminum aircraft fuselage panels that are joined by a stringer mounted on a rigid baffle (see Fig. 1). Two panels are necessary to allow wave transmission from one to the other when forced by convecting loads. The panel sizes are $0.65 \times 0.20 \times 0.001$ m, and the stringer cross section is 0.0128×0.0128 m. The test section is anechoically designed to study boundary-layer and sound interaction problems. The Reynolds number per meter Re/m of the turbulent boundary layer is 2.85×10^5, freestream velocity U_e is 46 m/s, and boundary-layer thickness is 0.060 m. The acoustic sources are created by four 120-W phase-amplitude matched speakers that are mounted on a diffuser within the anechoic sidewall and face the downstream panel (Fig. 1). The forcing frequency of the speakers is 960 Hz at the sound power level of 138 dB, which is needed to obtain chaotic response at the panel surface. The wall pressure fluctuation and the radiated pressure are measured by miniature pressure transducers, the flow velocity is measured by the hot-wire anemometer, and the panel vibration response is measured by miniature accelerometers. All measurements are made from direct current response.

Received March 24, 1997; presented as Paper 97-1688 at the AIAA/CEAS 3rd Aeroacoustics Conference, Atlanta, GA, May 12–14, 1997; revision received Nov. 18, 1997; accepted for publication Oct. 29, 1998.

*Senior Research Scientist, Fluid Mechanics and Acoustics Division. Associate Fellow AIAA.

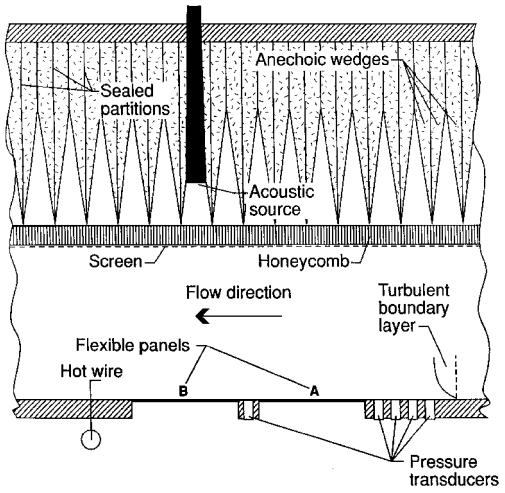

Fig. 1 Top view of wind tunnel setup with anechoic test section.

III. Transition from Periodic to Chaotic Responses

The tools used to analyze the dynamics of the responses of the panels and to characterize the oscillations forced by the turbulent boundary layer with or without pure tone sound are explained. The time history of the wall pressure fluctuation and panel acceleration is obtained. From the time history, the power spectral density, the phase portrait, and the probability distribution are computed. For a nonstationary signal $q(t, x)$, such as the pressure fluctuation $p(t, x)$ or the panel acceleration $g(t, x)$, the instantaneous power spectrum at instant T is defined by

$$P(f, T) = \left| \frac{1}{2\pi} \int_{T-I/2}^{T+I/2} \exp(i2\pi f t) q(t, x)\, \mathrm{d}t \right|^2$$

where T is chosen so that the experimental run contains the interval $T - I/2, T + I/2$ for a sufficiently large I. The probability density of $\hat{q}(T, x)$ is denoted by $Q(r, T)$, where

$$\hat{q}(T, x) = \frac{1}{I} \int_{T-I/2}^{T+I/2} q(t, x)\, \mathrm{d}t$$

$$Q(r, T) = \frac{\mathrm{d}}{\mathrm{d}r} \operatorname{prob}[\hat{q}(T, x) \le r]$$

In chaotic dynamics, searching for a low-dimensional characterization of the system is of great interest. Let $q(t, x)$ be a measured temporal signal or time series at position x, which is embedded in a d-dimensional phase space by a time delay τ. The set $Z(t) = [z_1(t), \ldots, z_d(t)]$ is regarded as a trajectory in the d-dimensional phase space. The distance between two points $Z(t_i)$ and $Z(t_j)$ is given by d_{ij}, and for a small $\varepsilon > 0$, let $N_d(n, \varepsilon)$ be the number of pairs of points with distance $d_{ij} < \varepsilon$. Then the correlation sum $C_d(\varepsilon)$ and the correlation dimension $D(d)$, for given d, are defined by Grassberger and Procaccia[15] as

$$C_d(\varepsilon) = \lim_{n \to \infty} \frac{2N_d(n, \varepsilon)}{n(n-1)}, \qquad D_d = \lim_{\varepsilon \to 0} \frac{\log C_d(\varepsilon)}{\log \varepsilon}$$

For computation, the parameters τ and d must be chosen properly, and the correlation dimension D_d is estimated by

$$D_d \approx \frac{\log C_d(n, \varepsilon)}{\log \varepsilon}$$

for some sufficiently small ε and large n. The estimate dimension D is taken as the asymptotic value of D_d as the embedding dimension d increases.

Given the estimated dimension D, the Lyapunov exponent, which is one of the most important characteristics in a dynamic system, can be computed approximately. Several methods exist for computing the Lyapunov exponents.[9,15–20] The Eckmann–Ruelle method[19] is used herein.

Consider $Z(t)$ as the trajectory of a dynamic system in the phase space of dimension $d = D$; obtain the tangent (linear) maps $T_i = 1, 2, \ldots, k$ of this reconstructed dynamical system by a least-squares fit; and decompose T_i into an orthogonal matrix Q_i and an upper triangular matrix by $T_1 - Q_1 R_1$ and $T_i Q_{i-1} = Q_i R_i$, for $i \ge 2$, and compute the Lyapunov exponents

$$\lambda_i = \lim \frac{1}{(k-1)} \log|(R_{k-1} \quad \cdots \quad R_2 R_1)_{ii}|$$

$$\text{for} \quad i = 1, 2, \ldots, D$$

For details see Appendices A and B and the Eckmann–Ruelle algorithm given by Conte and Dubois.[18]

Two classes of waves are present in the boundary layer and in the panel response: convecting waves along the direction of flow and nonconvecting waves occurring across the boundary layer originally predicted by Ribner.[21] The experimental observation of such waves was widely reported in the 1960s as space–time correction techniques.[22,23] The convecting waves are induced by turbulent eddies moving in the boundary layer that drive the panel oscillation. The correlation length, in the boundary layer along the direction of flow, is of the order of the boundary-layer thickness. For the panel, the surface waves propagate over several thicknesses.[23] The convected waves on the surface are merely their superposition of the effects of each cause in the presence of high-intensity sound. The response changes from linear to periodic and then to chaotic.[24,25] Table 1 lists the experimental stages used to analyze the wall pressure and panel responses.

A. Turbulent Boundary Layer Without and with Pure Tone Sound

At the upstream end of the test section, the boundary-layer thickness is artificially increased by putting sandpaper on the tunnel sidewall. As a result, the Reynolds number based on the boundary-layer thickness increases and becomes consistent in scale with current aircraft fuselage boundary layers. The structural size of the panels is typical of that used in aircraft fuselage sidewall panels. The mean velocity profiles of the turbulent boundary layer are measured at the downstream end of the second panel for the turbulent boundary layer alone and the turbulent boundary layer with the added pure tone sound at different amplitude levels. The results show that the turbulent boundary-layer thickness increases slowly as the sound power level increases.

The real-time wall pressure is measured at the center of the stringer supporting the two panels because the pressure transducer cannot be mounted on the panel without altering the response of the panel. The measured real-time pressure $p(t)$, the computed power spectral density $P(f, T)$, the phase plots of the computed $\dot{p}(t)$ vs $p(t)$, and the computed probability density $Q(r, T)$ are shown in Fig. 2a for a turbulent boundary layer without external sound and in Fig. 2b for a boundary layer with pure tone sound at 960 Hz and a sound power level of 138 dB. The real-time pressure $p(t)$, shown for an interval of 0.5 s in Figs. 2a and 2b near the instant T, is used for the evaluation of the instantaneous plots of spectrum, phase, and probability. The pressure fluctuations for Figs. 2a and 2b are significantly different because of the presence of pure tone sound.

Figure 2a shows a typical turbulent boundary-layer pressure fluctuation with the broadband spectrum, the phase portrait, and the nearly Gaussian distribution. Figure 2b shows the effect of added

Table 1 Panel forcing and response enroute to chaos

Force	Response (bifurcation state)
Turbulent boundary layer in absence of sound	Broadband, surface waves convecting with flow
Turbulent boundary layer with pure tone sound	Periodic with two or more commensurable frequencies superimposed on broadband, subharmonic response
Turbulent boundary layer with higher pure tone sound amplitude	Broadband chaos, panel displacement greater than panel thickness

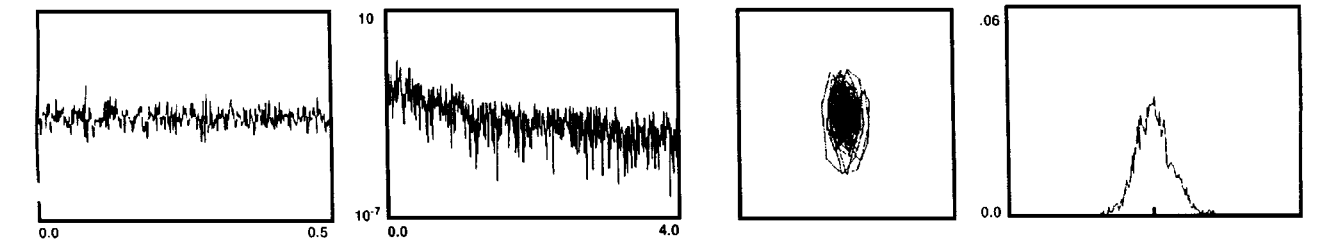

a) Turbulent boundary layer without external sound

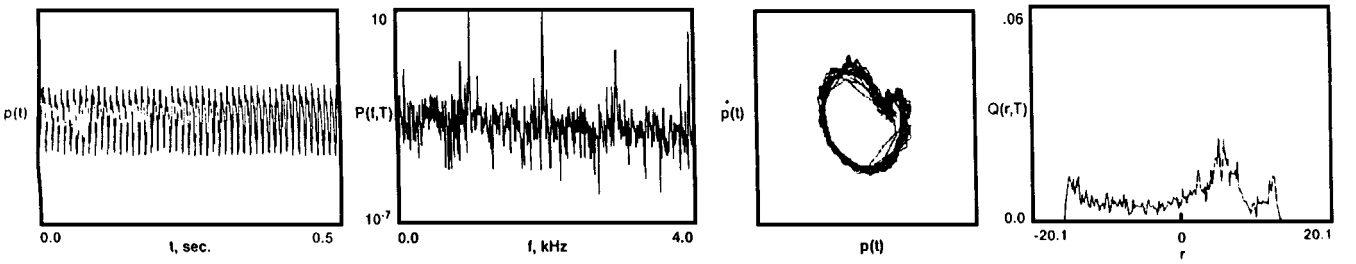

b) Turbulent boundary layer with external pure tone sound

Fig. 2 Normalized pressure fluctuation on stringer between two panels.

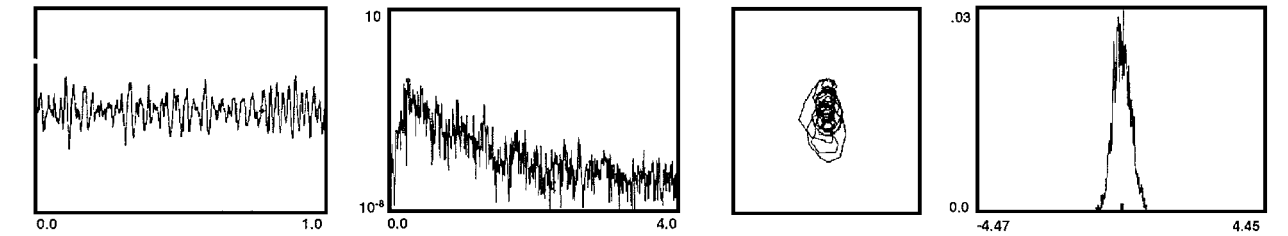

a) Turbulent boundary layer without external sound

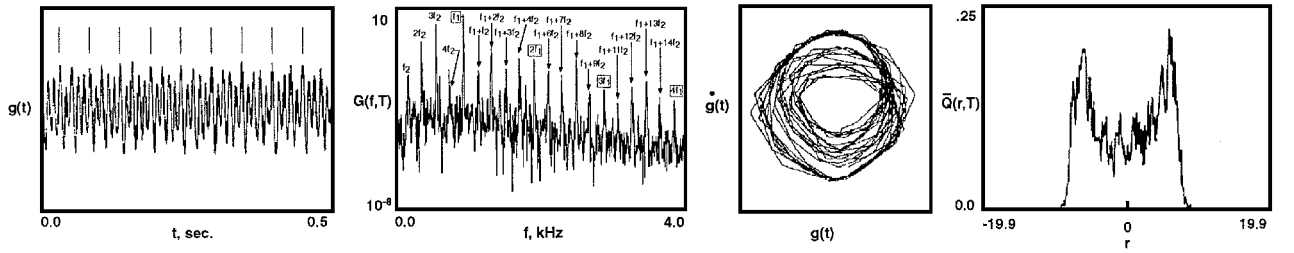

b) Turbulent boundary layer with external pure tone sound

Fig. 3 Panel normalized acceleration response.

pure tone sound to the level of 138 dB on the change of the amplitude of pressure fluctuation and the appearance of the peaks corresponding to the pure tone sound. In the spectrum plot, the peaks of the pure tone sound are almost 30 dB above the background level of the broadband with harmonics and subharmonics superimposed on the broadband spectrum. The amplitude of the broadband spectrum in Fig. 2b becomes nearly constant, whereas that in Fig. 2a is higher at the low-frequency end. This difference in broadband spectrum shows that the distribution of energy in the boundary layer is significantly altered by incident pure tone sound. The real-time pressure fluctuation shown in Fig. 2b consists mainly of N-wave-like oscillations of nearly constant amplitude, whereas the broadband fluctuation is not observable because of the larger scale needed for the N waves. In the phase portrait, the convective effect is overshadowed by the effect of the high-power-level sound at normal incidence. The probability plot is clearly non-Gaussian and has a much larger standard deviation than that in Fig. 2a.

B. Panel Response

The static pressure inside the wind tunnel is below the ambient pressure outside; this simulates aircraft panels in flight when the ambient pressure outside the fuselage is below the ambient pressure inside the cabin. Thus, the panels in the wind tunnel tend to deflect toward the moving stream. The mean static deflection is approximately the panel thickness or less. Because of the difficulty of mounting a pressure transducer on a moving surface without changing the inertia of the surface, the panel acceleration and displacement are measured instead. Also note that data taken with the displacement proximity probe become inaccurate as the displacement becomes of the order of the panel thickness. The spatial scale of the turbulent boundary layer is of the order of the boundary-layer thickness, $\frac{1}{8}$ of the panel length. Data are taken at $\frac{1}{4}$ panel lengths; two accelerometers at closer locations alter the response. Thus, we limit our results to a fixed point on the surface. Note that the panel acceleration is related to the load, that is, the wall pressure difference.

1. *Transition to Subharmonic Response*

The real-time acceleration response $g(t)$, measured on the centerline at $\frac{1}{4}$ panel length, is shown in Fig. 3a for a turbulent boundary layer without the incident pure tone sound and in Fig. 3b for a turbulent boundary layer with added pure tone sound at 960 Hz and a

sound power level of 130 dB for panel B. The time history of the response $g(t)$ in Fig. 3a shows a randomly modulated amplitude with a nearly Gaussian probability distribution $\bar{Q}(r, T)$. The power spectral density $G(f, T)$ and phase portrait $\dot{g}(t)$ vs $g(t)$ show typical random broadband response. Thus, the panel response shown in Fig. 3a is qualitatively similar to the wall pressure fluctuation without the incident sound in Fig. 2a.

In the spectrum plots, there are peaks of pure tone frequency, harmonics, and subharmonics. The subharmonics were absent in the earlier experiments for which the pure tone frequency and power level were lower. The quasiperiodic response and phase locking of two frequencies f_1 and f_2 are evident. The forcing frequency f_1 is 960 Hz. The spectral density shows the lowest subharmonic f_2 to be $f_1/5$. All peaks are linear combinations of f_1 and f_2. Thus, the phase and probability plots show periodic responses commensurable to f_1 and f_2. This observation is relevant to several recent developments in nonlinear dynamics.[8–11,22,23,25–31] A numerical and experimental study[24] was conducted on the response of a typical aircraft panel to time harmonic, plane acoustic waves at normal incident. By increasing the amplitude of the excitation source, the response of the panel changes from linear to chaotic. The route to chaos was found to be through a series of successive period-doubling bifurcations. The near-field and far-field pressures were measured and found to behave in a similar way.

2. Transition to Chaos

With increasing pure tone sound level interacting with the turbulent boundary layer, the panel oscillation loses its stability, a change from periodic to nonperiodic responses. By increasing acoustic power by 3 dB, the response becomes transient, alternating between quasiperiodic and chaotic with well-defined harmonic and nonharmonic peaks superimposed on a broadband signal (evidence of intermittency). Then by increasing the acoustic power by 9 dB, the response becomes fully chaotic.

For a 3-dB increase in acoustic power, the computed power spectra of the acceleration response from the measured real-time data at $\frac{1}{4}$ panel length are shown in Figs. 4a–4d. As time progresses from Figs. 4a to 4d, the spectra plots reveal nonstationary and nonlinear behaviors, whereas the remnants of the periodic behavior remain. Figure 4a indicates a small departure from the periodicity of Fig. 3b. Figures 4b and 4c indicate broadening of the spectra bandwidth about the major harmonic peaks superimposed on a broadband spectrum. As time progresses, further departure from periodicity is indicated because of the appearance of independent peaks superimposed on broadband as shown in Fig. 4d. Figures 4a–4d are examples of the panel response just above the threshold of periodicity. Sreenivasan,[10] in Fig. 4 of his paper, shows experimentally a similar broadening for a free shear layer wake due to a Reynolds number increase. He captures sequences of low-dimensional nonlinear behaviors in the initial stage of transition to turbulence, and he describes that the transition is characterized by a narrow window of chaos interspersed between regions of order. Above the threshold of periodicity, Figs. 4c and 4d of the present paper, a similar broadening trend is indicated.

At a higher pure tone sound level, a nonuniform rise in the broadband spectrum is observed in Figs. 5a–5c. The formally periodic responses of the time and phase data records, partially shown in Fig. 3b, become irregular, and the entire record appears nonperiodic. The corresponding phase data plots appear completely chaotic and intermixed with quasiperiodic oscillation diverging with time. The temporal responses indicate the existence of temporally varying finite amplitude waves. The spectra, as well as the probability plots, have broadband chaotic behaviors. Extended real-time response indicates spontaneous random switches of still different chaotic behaviors than were shown. The spontaneous switching seems to be the generalization of induced intermittency by the boundary-layer instability due to finite amplitude waves from the acoustic field. After a short period of time, the phase plots in Figs. 5a–5c never retrace themselves; this indicates that the motion is at incommensurable frequencies. From the data, we can establish that the combined turbulent boundary layer and high-level

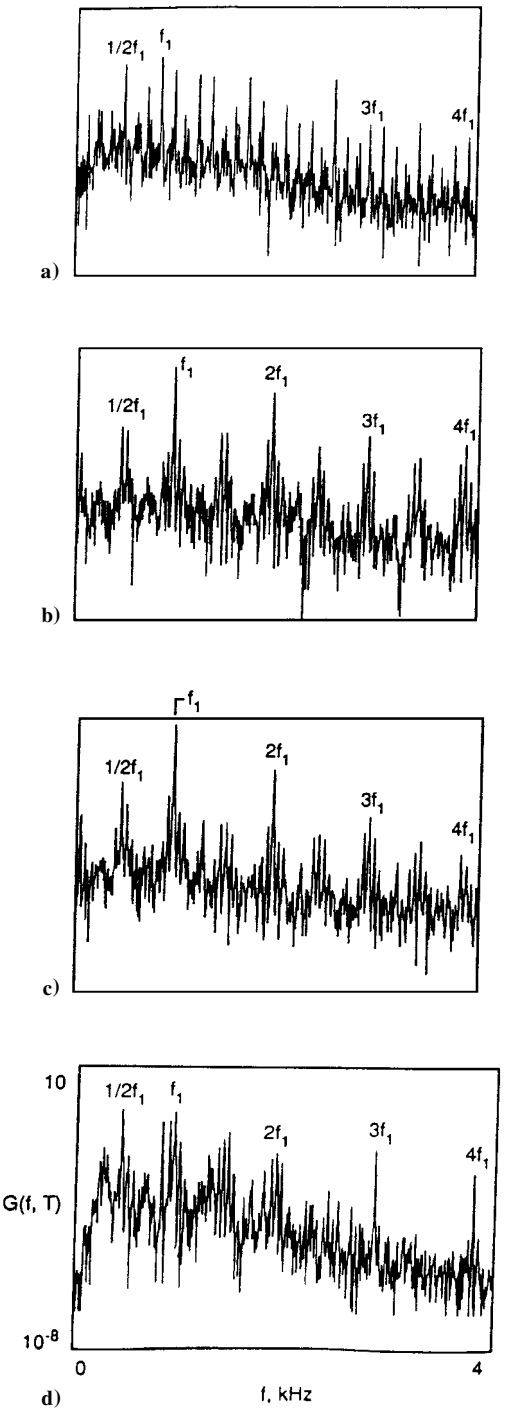

Fig. 4 Panel normalized acceleration response; transition to chaos.

pure tone sound are the sources that trigger chaotic behaviors. Additional experimental results by Gollub and Ramshanker,[3] Gollub and Benson,[4] and Matsumoto and Tsuda[32] have indicated that chaotic instability depends on the characteristics of the external noise field, a consideration well established and consistent with present results.[3,4,32,33]

Additional features of the wall pressure fluctuation and panel responses can be noted from the time histories in Figs. 2b and 5a–5c, which indicate that forcing and response are induced by a sequence of finite amplitude shock waves with expansion waves in between. The presence of shock waves is attributed to the high level of the acoustic pure tone impinging on the turbulent boundary layer, as shown clearly in the power spectrum plots. For practical consideration, the pure tone level is taken to be comparable with the sound level of a turbofan engine.

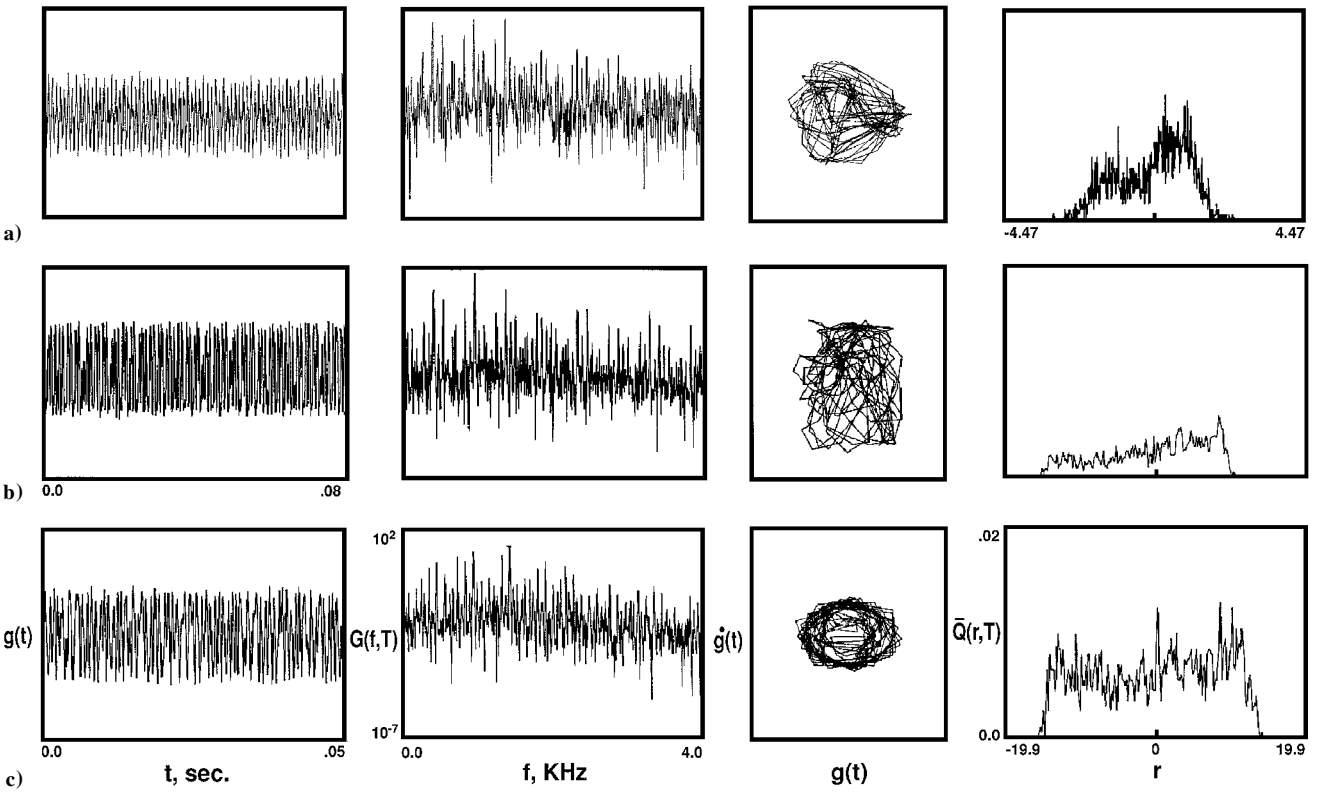

Fig. 5 Panel normalized acceleration response; turbulent boundary layer and external pure tone sound at successive time intervals.

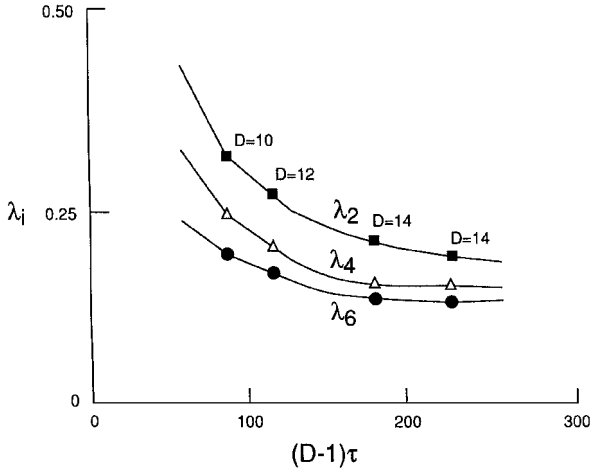

Fig. 6 Lyapunov exponent function of embedding time.

IV. Correlation Dimension and Lyapunov Exponents

The Grassberger and Procaccia[15] algorithm is used for the examination of the correlation dimension. The dimension of the attractor is related to the number of degrees of freedom of the panel response, as described by Ruelle[9] and Sreenivasan.[10] To compute the dimension, choose a range of size over which the scaling is to be estimated. The number of dimensions of the panel response increases with the increase in acoustic power level or flow speed or both. The computation procedures are shown in Appendices A and B.

Figure 6 shows the computed exponents, λ_2, λ_4, and λ_6, vs the embedding time $(D-1)\tau$ obtained from the temporal acceleration of the panel response of the time data in Fig. 5. Because the evaluated exponents are all positive, the results are consistent with experimental observations in Figs. 3–5, where changes in response from periodic to chaotic are shown as the input acoustic level superimposed on the turbulent boundary-layer increases. A positive Lyapunov exponent is sufficient proof that the attractor of the system is chaotic. Only the largest Lyapunov exponent is shown for the experimental data. As a conservative rule, 16 bits of precision are used for the exponent calculations. The number of orbits used for estimating λ varies between 20 and 40.

The preceding results give some information on the Lyapunov exponent of the temporal chaos at a point x. To compute the correlation dimension of the spatiotemporal chaos, we need multiple points $x = x_1, x_2, \ldots,$ and the computation becomes much more complicated.

V. Wave Transmitted Through Panels

The turbulent boundary layer induces panel vibration that in turn induces acoustic pressure in the ambient medium outside the tunnel, which simulates the cabin noise. A pressure tranducer is placed 0.79 m from the center of the downstream panel B outside the flowfield. To prevent acoustic interference, the exterior surface of panel A is covered with acoustic insulation material. Figure 7a shows the result of only turbulent boundary-layer panel loads, and Figs. 7b and 7c show turbulent boundary-layer and pure tone sound loads at the higher force amplitude (see Table 1). The plots include real-time history $p(t)$, power spectral density $P(f, T)$, phase $\dot{p}(t)$ vs $p(t)$, and probability density distribution $\tilde{Q}(r, T)$. The pressure transmitted by the panel forced by the turbulent boundary layer is broadband, similar to the wall pressure fluctuation and the vibration response with a Gaussian-type probability distribution. The transmitted pressure in the presence of high-level pure tone sound is also broadband with a superimposed N-wave field that originated from the wall pressure load (Fig. 2b) and is transmitted by the panel motion (Figs. 5a–5c). The power spectral densities are chaotic. The probability distributions of the transmitted pressures are non-Gaussian, and the phases vary from chaotic to quasiperiodic. Like the panel response, the amplitude of the transmitted pressure changes with time over a wide range of chaotic behavior as indicated in Figs. 7b and 7c. The acoustic pressure is nonsymmetrical with respect to the panel center, similar to the panel response. Thus, nonlinear acoustic waves have practical applications to the simulation of cabin noises in addition to theoretical interest.

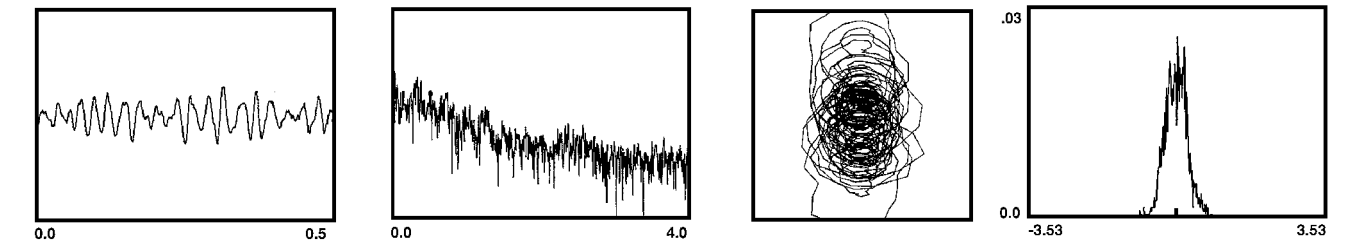

a) Turbulent boundary layer without external sound

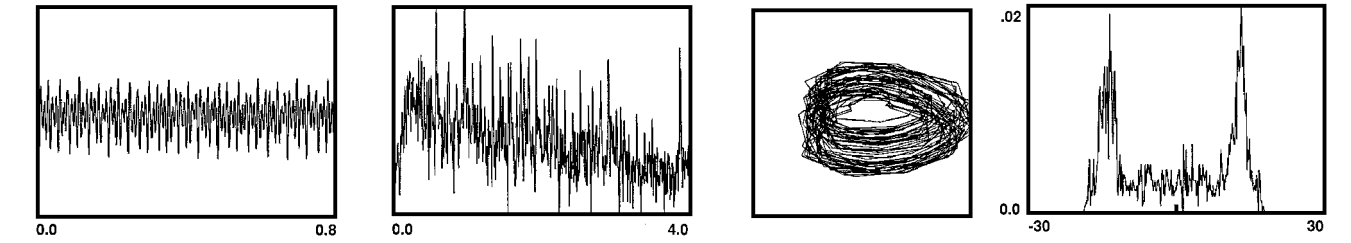

b) Turbulent boundary layer with external sound at successive time intervals

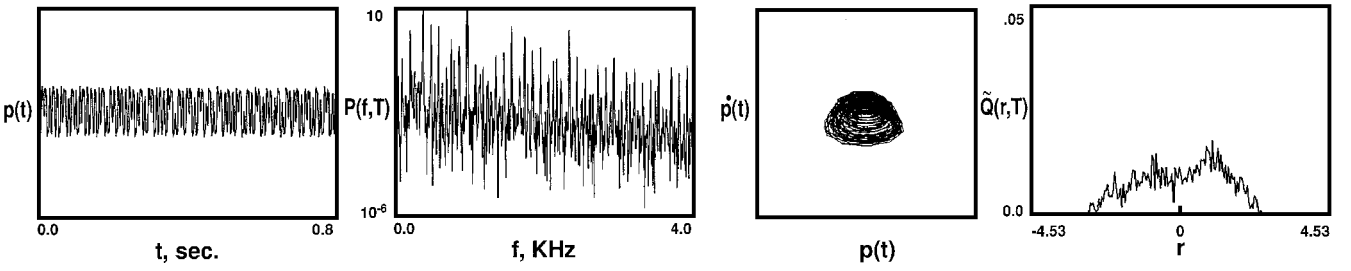

c) Pure sound tones at successive time intervals

Fig. 7 Normalized panel transmitted pressure.

VI. Discussion and Conclusions

Temporal evaluation of periodic or chaotic panel responses forced by the turbulent boundary layer and a pure tone sound was investigated to study sequences of transition of dynamic behavior as the pure tone sound level increases. From an initial state, the turbulent boundary-layer flow with superimposed pure tone sound causes the response of the panel to go through a reproducible sequence of subharmonic bifurcations in the first stage as the tone level is increased; when the level exceeds a critical value, the response of the panel goes through breaking of the period doubling in the final stage. In particular, the following behaviors were observed as the sound level increased:

1) The wall pressure fluctuation and the turbulent boundary layer were altered by the pure tone sound. The pure tone and harmonics levels exceeded the broadband level by 30 dB in sound power level; this was accompanied by a reduction of the lower frequency broadband levels. As a result the pure tone sound coupled with the turbulent boundary layer modified the boundary-layer thickness, the spatial correlation, and the load on the structure.

2) The coupling between the acoustic load and the turbulent boundary-layer load on the panel induced a quasiperiodic response to the panel. The periodic response was composed of two coupled attracting regions, where the trajectories made transition from one to the other through the commensurable subharmonic frequencies f_2 coupled to the force frequency f_1. As a result, the power spectral density had a series of peaks at all integer combinations of two commensurable frequencies f_1 and f_2. Any other choice of reference frequency was related to these two frequencies.

3) As the level of the pure tone increased, the panel response bifurcated from quasiperiodicity to chaos. Estimation of positive Lyapunov exponents from experimental time series provided quantitative characterization of the panel dynamic behavior. One significant feature was that the response was not steady but randomly changed from chaotic to quasiperiodic. The continuous variation was an indication that the responses had nonstationary statistics because the nonperiodic responses had no steady average.

The dynamics may be similar to the observation made by Gollub and Benson[4] in which phase locking convection alternates between quasiperiodic and periodic responses. The wave field behaves somewhat like the turbulent boundary-layer pressure field; the localized acoustic load introduces changes in amplitude and in distribution. The combined turbulent boundary-layer and acoustic loads cause an increase in complexity so that the response field becomes transient and dispersive. In spite of recent results, the whole nonlinear-nonstationary problem in structural dynamics is still not satisfactorily understood. Control of chaos caused by turbulent boundary layer and sound on a panel is more complicated than that of the periodic responses.

Appendix A: Computing Correlation Dimension D

The correlation dimension D is computed as follows:

1) Given nonstationary signal at x, $q(t, x)$, consider

$$z_1(t) = q(t, x), \qquad z_2(t) = q(t+\tau, x), \ldots$$

$$z_d(t) = q[t + (d-1)\tau, x]$$

where τ is a properly chosen time delay (for some time greater than correlation time).

2) Form a d-dimensional (pseudo)phase space S and consider $Z(t) = [z_1(t), \ldots, z_d(t)]$ as a trajectory Γ in S.

3) Discretize the time $k = t_0 < t_1 \ll t_n$. Choose the dimension $d = 2, 3, \ldots$, of the embedding phase space S (depending on the unknown size of the strange attractor), and compute $Z_n(t_i)$, for $i = 1, 2, \ldots, n$.

4) Compute the distances d_{ij}:

$$d_{ij} \| Z(t_i) - Z(t_j) \| = \sqrt{\sum_{k=1}^{n} [z_k(t_i) - z_k(t_j)]^2}, \quad \text{for} \quad 1 \le i < j \le n$$

5) For a given $\varepsilon > 0$, count how many pairs of (i, j) with $1 \le i < j \le m$ have distance

$$d_{ij} < \varepsilon$$

Denote this number by $N_d(n, \varepsilon)$.

6) The correlation sum C_d and the correlation dimension D_d are defined as

$$C_d(\varepsilon) = \lim_{n\to\infty} 2\frac{N_d(n,\varepsilon)}{n(n-1)}, \qquad D_d = \lim_{\varepsilon\to 0}\frac{\log C_d(n,\varepsilon)}{\log\varepsilon}$$

for some sufficient small ε and large n.

7) Because it is unknown how large d should be chosen, logically start with $d = 2, 3, 4, \ldots$, and see the trends of the numerical results.

Appendix B: Computing the Lyapunov Exponents

Apply the Eckmann–Ruelle algorithm[18,19] to compute the Lyapunov exponents. This algorithm consists of the implementation of the following steps:

1) Based on the estimated dimension D, set the dimension of the phase space $d = D$. Consider $Z(t)$ as a trajectory in this phase space.

2) Set $t_i = i\Delta t$, for $i = 1, 2, \ldots, n$, and $\tau = p\Delta t$, where p is an integer. This gives rise to

$$Z_i = Z(t_i), \qquad \text{for} \qquad i = 0, 1, \ldots, (n, p) = k$$

which is assumed to evolve according to

$$Z_{i+1} = F(Z_i), \qquad \text{for} \qquad i = 0, \ldots, k$$

3) Approximate the nonlinear map F by a piecewise linear (tangent) map T_i,

$$(Z_{i+1} - Z_i) = F(Z_i) - F(Z_{i-1}) \approx T_i(Z_i - Z_{i-1}) \qquad \text{for} \qquad i = 0, r, \ldots, (k-1)$$

where T_i is determined by a least-squares method with respect to a set of neighboring points of Z_i, with the distance r, for suitably chosen r.

4) Decompose the matrix T_i into an orthogonal matrix Q_i and an upper triangular matrix R_i by the QR factorization as follows:

$$T_1 = Q_1 R_1$$

$$T_2 Q_1 = Q_2 R_2$$

$$\vdots$$

$$T_i Q_{i-1} = Q_i R_i, \qquad \text{for} \qquad i = 2, 3, \ldots, k-1$$

5) Compute the product matrix

$$R^{(k)} = (R_{k-1} \quad \cdots \quad R_2 R_1)$$

with the entry

$$\left(R^{(k)}\right)_{ij} = r_j^{(k)}, \qquad \text{for} \qquad i \cdot j = 1, \ldots, D$$

6) Compute the Lyapunov exponents

$$\lambda_i = \lim\frac{1}{(k-1)}\log|(R_{k-1} \quad \cdots \quad R_2 R_1)_{ii}| \qquad \text{for} \quad i = 1, 2, \ldots, D$$

$$\approx \frac{1}{k-1}\log|(R_{k-1} \quad \cdots \quad R_2 R_1)_{ii}|$$

The principal Lyapunov exponent $\lambda = \max_i \lambda_i$.

References

[1]Maestrello, L., "Control of Panel Response to Turbulent Boundary Layer and Acoustic Excitation," *AIAA Journal*, Vol. 34, No. 2, 1966, pp. 259–264.

[2]Maestrello, L., "Active Control of Panel Oscillation Induced by Accelerated Turbulent Boundary Layer and Sound," *AIAA Journal*, Vol. 35, No. 5, 1997, pp. 796–801.

[3]Gollub, J. P., and Ramshanker, R., "Spatiotemporal Chaos in Interfacial Waves," *New Perspectives in Turbulence*, edited by L. Sirovich, Springer–Verlag, Berlin, 1991, pp. 165–194.

[4]Gollub, J. B., and Benson, S. V., "Many Routes to Turbulent Convection," *Journal of Fluid Mechanics*, Vol. 100, 1980, pp. 449–471.

[5]Hohenberg, P. C., and Shraiman, B. I., "Chaotic Behavior of an Extended System," *Physica*, Vol. D37, July 1989, pp. 109–115.

[6]Chate, H., and Manneville, P., "Spatiotemporal Intermittency," *Turbulence—A Tentative Dictionary*, edited by P. Tabeling and O. Cardoso, Plenum, New York, 1995, pp. 111–116.

[7]Gassmann, F., "Noise-Induced Chaos-Order Transition," *Physical Review E*, Vol. 55, No. 3, 1997, pp. 2119–2123.

[8]Sahay, A., and Sreenivasan, K. R., "The Search for a Low-Dimensional Characterization of a Local Climate System," *Philosophical Transactions of the Royal Society of London*, Vol. A354, July 1996, pp. 1715–1750.

[9]Ruelle, D., "The Claude Bernard Lecture, 1989, Deterministic Chaos: The Science and Fiction," *Proceedings of the Royal Society of London*, Vol. A472, Feb. 1990, pp. 241–248.

[10]Sreenivasan, K. R., "Transition and Turbulent in Fluid Flow and Low-Dimensional Chaos," *Frontier in Fluid Mechanics*, edited by S. H. Davis and J. M. Lumley, Springer–Verlag, Berlin, 1985, pp. 41–67.

[11]Giglio, M., Musazzi, S., and Perini, U., "Transition to Chaotic Behavior via a Reproducible Sequence of Periodic-Doubling Bifurcations," *Physical Review Letters*, Vol. 47, No. 4, 1981, pp. 243–246.

[12]Abarbanel, H. D. I., *Analysis of Observed Chaotic Data*, Springer–Verlag, Berlin, 1996, pp. 25–112.

[13]Newhouse, D., Ruelle, D., and Takens, F., "Occurrence of Strange Axiom A Attractors Near Quasi Periodic Flows on $T^m \geq 3$," *Communication in Mathematics and Physics*, Vol. 64, No. 1, 1978, pp. 35–40.

[14]Dowell, E. H., "Chaotic Oscillations in Mechanical Systems," *Computational Mechanics*, Vol. 3, Springer–Verlag, Berlin, 1988, pp. 199–216.

[15]Grassberger, P., and Procaccia, I., "Measuring the Strangeness of Strange Attractors," *Physica D*, Vol. 9, No. 1–2, 1983, pp. 189–208.

[16]Abarbanel, D. I., Brown, R., and Kadtke, J. B., "Prediction and System-Identification in Chaotic Nonlinear-System-Time-Series with Broadband Spectra," *Physics Letters A*, Vol. 138, No. 8, 1989, pp. 401–408.

[17]Aguirre, L. A., and Billings, S. A., "Validating Identified Nonlinear Models with Chaotic Dynamics," *International Journal of Bifurcation and Chaos in Applied Sciences and Engineering*, Vol. 4, No. 1, 1994, pp. 109–126.

[18]Conte, R., and Dobois, M., "Lyapunov Exponents of Experimental System," *Nonlinear Evolutions*, edited by J. P. D. Leon, World Scientific, Singapore, 1988, pp. 767–780.

[19]Eckmann, J. P., and Ruelle, P., "Ergotic Theory Strange Attractor," *Reviews of Modern Physics*, Vol. 57, No. 3, Pt. 1, 1985, pp. 617–656.

[20]Eckmann, J. P., Kamphorst, S. O., Ruelle, D., and Ciliberto, S., "Lyapunov Exponents for Time Series," *Physical Review A: General Physics*, Vol. 34, No. 6, 1986, pp. 4971–4979.

[21]Ribner, H. S., "Boundary Layer Induced Noise in the Interior of Aircraft," Inst. of Aerophysics, Rept. 37, Univ. of Toronto, Toronto, ON, Canada, 1958.

[22]El Baroudi, M., "Turbulence Induced Panel Vibration," Univ. of Toronto Inst. of Aerospace Science, UTIAS Rept. 98, Toronto, ON, Canada, 1964.

[23]Maestrello, L., "Fuselage Structure Response to Boundary Layer, Tonal Sound, and Jet Noise," AIAA Paper 98-2276, May 1998.

[24]Maestrello, L., Frendi, A., and Brown, D. E., "Nonlinear Vibration and Radiation from a Panel with Transition to Chaos Induced by Acoustic Waves," *AIAA Journal*, Vol. 30, No. 11, 1992, pp. 2632–2637.

[25]Chow, P. L., and Maestrello, L., "Stabilization of Non-Linear Panel Vibration by Boundary Layer Damping," *Journal of Sound and Vibration*, Vol. 182, No. 4, 1995, pp. 541–558.

[26]Hilborn, R. C., *Chaos and Nonlinear Dynamics*, Oxford Univ. Press, Oxford, England, UK, 1994, Chap. 4.

[27]Hurre, P., and Monkewitz, P. A., "Local and Global Instabilities in Spatially Developing Flow," *Annual Review of Fluid Mechanics*, Vol. 22, 1990, pp. 473–537.

[28]Flesselles, J. M., Croquette, V., and Jucquois, S., "Periodic Doubling of a Torus in a Chain of Oscillators," *Physical Review Letters*, Vol. 72, No. 18, 1994, pp. 2871–2874.

[29]Von Stamm, J., Gerdts, U., Buzug, T., and Pfister, G., "Symmetry Breaking and Period Doubling on a Torus in the VLF Regime in Taylor-Couette Flow," *Physical Review E*, Vol. 54, No. 5, 1996, pp. 4938–4957.

[30]Dowell, E. H., and Pezeshki, C., "On the Understanding of Chaos in Duffing Equation Including a Comparison with Experiment," *Journal of Applied Mechanics*, Vol. 53, No. 1, 1986, pp. 5–9.

[31]Franceschini, V., "Bifurcations of Tori and Phase Locking in a Dissipative System of Differential Equations," *Physica D*, Vol. 6, No. 3, 1983, pp. 285–304.

[32]Matsumoto, J. C., and Tsuda, I., "Noise-Induced Order," *Journal Statistical Physics*, Vol. 31, No. 87, 1983, pp. 87–106.

[33]Sirovich, L., Ball, K. S., and Keefe, L. R., "Plane Waves on Structures in Turbulent Channel Flow," *Physics of Fluids*, Vol. A2, No. 12, 1990, pp. 2217–2226.

S. Glegg
Associate Editor